Detection of manoeuvring low SNR objects in receiver arrays

Detection of manoeuvring low SNR objects in receiver arrays

Kimin Kim, Murat Üney and Bernard Mulgrew
Institute for Digital Communications, School of Engineering,
The University of Edinburgh, EH9 3JL, Edinburgh, UK
Emails:{K.Kim, M.Uney, B.Mulgrew}@ed.ac.uk

***Abstract*—In this work, we are interested in detecting manoeuvring objects in high noise background using an active sensor with a uniform linear array (ULA) receiver and propose a joint pulse integration and trajectory estimation algorithm. This algorithm allows us to detect low SNR objects by integrating multiple pulse returns while taking into account the possibility of object manoeuvres. In the proposed algorithm, the detection is performed by a Neyman-Pearson test, i.e., a likelihood ratio test. The likelihood function used in this test accommodates the radar ambiguity function evaluated in accordance with object related parameters such as location, velocity and reflection coefficient. The trajectory estimation is performed by Bayesian recursive filtering based on the state model of the location and velocity parameters. The reflection coefficient is estimated by a maximum likelihood (ML) estimator. These estimates are used in pulse integration, leading to coherent integration during a coherent processing interval (CPI) and non-coherent integration across consecutive CPIs. We also compare the proposed algorithm with conventional techniques.**

I. Introduction

Detection of manoeuvring objects in a relatively high noise background is a challenging task and a highly desired capability in wide area surveillance applications. In these applications, active sensor systems, for example radar systems, are often used. Detection in active sensing involves transmitting modulated pulse trains towards the surveillance region, and, testing the hypothesis that the received signal contains reflected versions of the transmitted waveforms against the noise only signal hypothesis. The received signal varies with object related parameters such as range (equivalently, time of flight), velocity (equivalently, doppler shift) and effective reflection coefficient. The data for testing object existence consists of samples obtained after correlating (or, matched filtering) this signal with expected waveforms corresponding to selected values of these parameters [1, Chp.1]. Equivalently, the range-bearing and doppler space is uniformly separated into bins.

For low SNR objects, the reflected pulse energy is on a level very similar to the noise background. This makes detection difficult because a single measurement set (i.e., the data set for a single emitted pulse) is likely to fail in providing sufficient evidence of object existence. For this reason, multiple measurements (i.e., data sets for multiple pulse returns) need to be considered by summing up the reflected pulse energy across them, which is often referred to as pulse integration. In principle, prolonging the integration time increases the chances that a low SNR object can be detected. Conventional pulse integration such as coherent integration and non-coherent integration (see, e.g, [1, Chp.6]), however, perform integration for the same bins without taking into account the possibility of object movements across them. This leads to failure in collecting all the evidence contained in the received signals over time when the object is manoeuvring. An alternative is to use matched filters that are tuned to various trajectories [2], however, the number of filters required easily becomes excessive with increasing integration time.

It is possible to perform long time integration, on the other hand, by estimating the object trajectory and selecting data samples for pulse integration accordingly. This corresponds to adaptive synthesis of matched filters tuned to trajectories, in a sense. Trajectory estimation based on the data used for pulse integration is often referred to as track-before-detect (see, for example [3], [4]). These algorithms often use the modulus of the complex data sampled with pulse-width period and assume that the statistics of the reflection coefficient is known. It is desirable to estimate this quantity, however, this requires more samples than one can collect at this sampling rate within a coherent processing interval (CPI) [5]. Moreover, in [6], it is argued that taking the phase of the complex reflection coefficient into account improves the detection performance. An algorithm which uses both the modulus and the phase of the data, i.e., the complex data, collected with a sampling rate much higher than the aforementioned rate is proposed in [7]. This scheme performs long time integration by simultaneously estimating the reflection coefficient and range of the reflector position along a bearing line.

In this work, we consider a uniform linear array (ULA) receiver and propose a joint pulse integration and trajectory estimation algorithm, which uses complex data sampled with pulse-width period. The data captures spatio-temporal information and is stacked as a cube of range, bearing and doppler bins. The reflection coefficient within a CPI is estimated using a maximum likelihood approach. This quantity is used in the likelihood for trajectory estimation as well as pulse integration. The ULA structure allows us to estimate the reflection coefficient with favourable accuracy using the limited amount of data available in a CPI. As a result, coherent processing takes place within a CPI followed by non-coherent integration across consecutive CPIs. This approach results in an integrated value close to the best achievable using true trajectory.

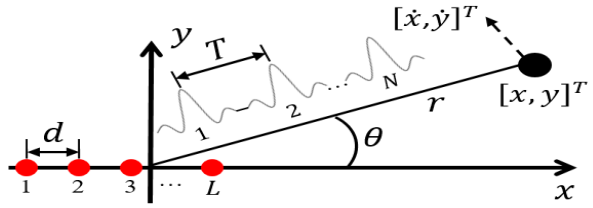

Fig. 1. Illustration of the problem scenario with a ULA (red dots) centered at the origin of the Cartesian plane and a low SNR object at $[x, y]^T$ with velocity $[\dot{x}, \dot{y}]^T$.

Section II of this article gives details of the scenario considered and the problem definition. In Section III, we introduce the proposed algorithm which involves trajectory estimation, and, derive the maximum likelihood estimator for the reflection coefficient that is required for tracking. In Section IV, we demonstrate the proposed algorithm in an example scenario and conclude in Section V.

II. Problem Statement

We consider a transmitter that emits N pulses followed by silent periods towards a surveillance region. These pulses are reflected back by objects in this region. We assume that the reflectors remain coherent in this time interval, also known as a coherent processing interval (CPI). A ULA receiver co-located with the transmitter receives the reflected versions of the transmitted waveforms with additive noise. This receiver consists of L elements spaced with d distance. The reflections are characterised by the reflector kinematic state $X = [x, y, \dot{x}, \dot{y}]^T$, where $[x, y]^T$ is the location in 2D Cartesian coordinates, $[\dot{x}, \dot{y}]^T$ is velocity, and $(.)^T$ denotes transpose. This scenario is illustrated in Fig. 1.

A. Signal model

For a reflector with kinematic parameters X, the corresponding signal is characterised by a spatial steering vector $s_s(\theta)$ and a temporal vector $s_t(r, \omega_d)$, where (θ, r) is the polar coordinates of the point $[x, y]^T$ in Cartesian coordinates, i.e.,

$$\theta = \tan^{-1}\left(\frac{y}{x}\right), \; r = \sqrt{x^2 + y^2}.$$

ω_d is the doppler angular frequency given by

$$\omega_d = \frac{4\pi}{\lambda_c}\left(\dot{x}\cos(\theta) + \dot{y}\sin(\theta)\right),$$

where λ_c is the carrier wavelength.

The spatial steering vector is specified by the geometry of the ULA

$$s_s(\theta) = [1, \exp\left(-j\omega_c \frac{d}{c}\sin(\theta)\right), \ldots, \exp\left(-j\omega_c (L-1)\frac{d}{c}\sin(\theta)\right)]^T, \quad (1)$$

where d is the internal element spacing, L is the number of elements in the array, $\omega_c = 2\pi f_c$ is the carrier angular frequency, and c is the speed of light.

The temporal vector $s_t(r, \omega_d)$ is given by

$$s_t(r, \omega_d) = [\exp\left(-j\omega_c \frac{2r}{c}\right), \exp\left(-j\omega_c \frac{2r}{c}\right)\exp(j\omega_d T), \ldots, \exp\left(-j\omega_c \frac{2r}{c}\right)\exp\left(j\omega_d (N-1)T\right)]^T, \quad (2)$$

where T is pulse repetition interval (PRI), i.e., the time period between the N pulses. In the forward signal model for the ULA, the spatial and temporal vectors are combined as

$$s(\theta, r, \omega_d) = s_s(\theta) \otimes s_t(r, \omega_d), \quad (3)$$

where $\otimes$ denotes the Kronecker product operator.

The reflections in the received signal of the ULA are searched by matched filtering, which computes the correlation of the transmitted waveform with the received signal. The filter output is sampled in fast time which uniformly divides the range space into range bins of width Δr. Doppler space is also discretised with $\Delta\omega_d$ steps as well as the bearing space which is sampled with steps $\Delta\theta$. As a result, the data vector in a CPI under the hypothesis that a reflector exists in the $i = [i_1, i_2, i_3]$th bearing-range-doppler bin with an unknown reflection coefficient A is found as

$$Z(i) = A s(i_1\Delta\theta, i_2\Delta r, i_3\Delta\omega_d) + n, \quad (4)$$

where $s(.)$ is given by (3), $n \sim \mathcal{CN}(.; \mathbf{0}, \sigma^2\mathbf{I})$ is additive white complex Gaussian noise vector, and A is an unknown complex constant. The data vector $Z_k(i)$ at the k^{th} CPI is hence

$$Z_k(i) = \begin{cases} A_k s_k(i_1\Delta\theta, i_2\Delta r, i_3\Delta\omega_d) \\ \quad + n_k(i_1, i_2, i_3) & , H_1 \text{ holds}, \\ n_k(i_1, i_2, i_3) & , H_0 \text{ holds}, \end{cases} \quad (5)$$

where H_1 is the hypothesis that a reflector exists in the i^{th} bin, H_0 is the null hypothesis, and, $k = 1, \ldots, K$ indexes integration over K CPIs.

B. Problem definition

Our goal is to decide on the existence of an object moving along a trajectory $X_{1:K}$. We use the Neyman-Pearson test [8, Chp.3] which is a likelihood ratio test, for this purpose. The input to the test is the set of complex measurement vectors $\{Z_k(i_k)\}_{k=1:K}$, where $i_k = [i_{k,1}, i_{k,2}, i_{k,3}]$ corresponds to the bearing-range-doppler bin associated with $(\theta_k, r_k, \omega_{d_k})$ of X_k.

The likelihood ratio test for an object with the trajectory $X_{1:K}$ is then given by

$$L(Z_{1:K}(i_{1:K})|X_{1:K}, A_{1:K}) \underset{H_0}{\overset{H_1}{\gtrless}} \mathcal{T}_K \quad (6)$$

where the ratio L of the likelihood for the object existence hypothesis and the likelihood for the noise only signal hypothesis factorises over time as

$$L(Z_{1:K}(i_{1:K})|X_{1:K}, A_{1:K}) = \prod_{k=1}^{K} L_k(Z_k(i_k)|X_k, A_k) = \prod_{k=1}^{K} \frac{l(Z_k(i_k)|X_k, A_k, H_1)}{l(Z_k(i_k)|H_0)}, \quad (7)$$

where L_k denoting the likelihood ratio at the k^{th} CPI. The numerator and denominator in (7) –considering (5)– are found as

$$l(Z_k(i_k)|X_k, A_k, H_1) = \left(\frac{1}{\pi\det(\sigma^2\mathbf{I})}\right)\exp\left(\frac{-|Z_k(i_k) - A_k s_k(\theta_k, r_k, \omega_{d_k})|^2}{\sigma^2\mathbf{I}}\right), \quad (8)$$

$$l(Z_k(i_k)|H_0) = \left(\frac{1}{\pi \det(\sigma^2\mathbf{I})}\right) \exp\left(\frac{-|Z_k(i_k)|^2}{\sigma^2\mathbf{I}}\right), \quad (9)$$

where $\sigma^2\mathbf{I}$ is the noise covariance. An explicit expression for the instantaneous likelihood ratio in (7) is obtained after substituting from (8) and (9) as follows,

$$L_k(Z_k(i_k)|X_k, A_k) = \exp\left(\frac{-|Z_k(i_k) - A_k s_k(\theta_k, r_k, \omega_{d_k})|^2 + |Z_k(i_k)|^2}{\sigma^2\mathbf{I}}\right). \quad (10)$$

The problem we consider is simultaneous estimation of $X_{1:K}$ and evaluation of the likelihood ratio test in (6) by evaluating (7)–(10) for $k = 1, \ldots, K$. Note that, this also involves estimation of the reflection coefficient $A_{1:K}$ and specification of the test threshold $\mathcal{T}_K$, as well. Estimation of all of these parameters, specification of a constant false alarm rate (CFAR) threshold and evaluation of the test are detailed in Section III.

III. Joint pulse integration and trajectory estimation

A. Trajectory estimation using coherent returns

Let us consider object trajectory (i.e., the kinematic parameters) estimation using coherent returns. For estimating the kinematic parameters $X_{1:K}$, we use a Markov state space model and perform Bayesian recursive filtering given by the following prediction and update recursions:

$$\begin{aligned} p(X_k|Z_{1:k-1}) &= \int p(X_k|X_{k-1}) p(X_{k-1}|Z_{1:k-1}) dX_{k-1} \quad (11)\\ p(X_k|Z_{1:k}) &\propto p(Z_k|X_k, A_k) p(X_k|Z_{1:k-1}), \end{aligned}$$

where $p(X_k|Z_{1:k})$ is the posterior probability density function of the object state, $p(Z_k|X_k, A_k)$ is the measurement likelihood, and, $p(X_k|X_{k-1})$ is the Markov transition density of the object state X_k.

The measurement likelihood is given by

$$\begin{aligned} p(Z_k|X_k, A_k) &= l(Z_k(i_k)|X_k, A_k) \prod\nolimits_{j \neq i_k} l(Z_k(j)|H_0) \\ &\propto L_k(Z_k(i_k)|X_k, A_k), \quad (12) \end{aligned}$$

where the second line follows after dividing both parts of the first equality by the product of the noise-only hypothesis likelihood for all range-bearing-doppler bins. Therefore, we use the following update for filtering

$$p(X_k|Z_{1:k}) \propto L_k(Z_k(i_k)|X_k, A_k) p(X_k|Z_{1:k-1}). \quad (13)$$

The object dynamic model is selected as a random acceleration model, i.e.,

$$X_k = F X_{k-1} + b_{k-1}, \quad F \triangleq \begin{bmatrix} 1 & 0 & \Delta & 0 \\ 0 & 1 & 0 & \Delta \\ 0 & 0 & 1 & 0 \\ 0 & 0 & 0 & 1 \end{bmatrix} \quad (14)$$

where b_{k-1} is process noise (modelling manoeuvres), which is zero-mean Gaussian with a known covariance $\mathbf{\Sigma}$, and Δ is the time interval at each sate between two consecutive CPIs. Hence, $p(X_k|X_{k-1}) = \mathcal{N}(X_k; FX_{k-1}, \mathbf{\Sigma})$.

We use a sequential Monte Carlo (SMC) realisation of Bayesian recursive filtering known as the particle filter [9]. Particle filters propagate weighted samples of probability densities in order to represent them. In particular, we use the bootstrap filtering approach: Given a set of particles $\{X_{k-1}^{(j)}, \zeta_{k-1}^{(j)}\}_{j=1}^{M}$ representing the posterior in (13) at time $k-1$, we obtain particles for the prediction density in (11) by sampling from the Markov transition, and obtain M particles $\{X_k^{(j)}, \zeta_{k-1}^{(j)}\}_{j=1}^{M}$ with $X_k^{(j)} \sim p(.|X_{k-1}^{(j)})$.

Then, the posterior at k is represented by $X_k^{(j)}$s with weights updated using the likelihood ratio given in (10), i.e.,

$$\begin{aligned} \zeta_k^{(j)} &= \frac{\tilde{\zeta}_k^{(j)}}{\sum_{i=1}^{M} \tilde{\zeta}_k^{i}}, \quad (15)\\ \tilde{\zeta}_k^{i} &\propto \zeta_{k-1}^{(j)} L_k(Z_k(i_k^{(j)})|X_k^{(j)}, A_k^{(j)}). \end{aligned}$$

Given the posterior weighted particles, the estimated state at the k^{th} CPI based on the measurements $Z_{1:k}$ is given by

$$\hat{X}_k \triangleq \sum_{j=1}^{M} \zeta_k^{(j)} X_k^{(j)}. \quad (16)$$

We check the weighted particles for degeneracy after normalising the weights (see, e.g., [9]). The degeneracy test N_{eff} is conducted by

$$N_{eff} = \frac{1}{\sum_{i=1}^{M} {\zeta_k^{(j)}}^2} < \mathcal{B}, \quad (17)$$

where $\mathcal{B}$ is the minimum number of effective particles allowed. We perform re-sampling (with replacement) whenever the condition in (17) is met.

B. Maximum likelihood estimator for the reflection coefficient

Let us consider the estimation of $A_k^{(j)}$ for evaluating the likelihood of the object existence hypothesis. Given the object state $X_k^{(j)}$, we use a maximum likelihood (ML) estimation approach by solving

$$\hat{A}_k^{(j)} = \arg\max_{A_k^{(j)}} \log l(Z_k(i_k^{(j)})|X_k^{(j)}, A_k^{(j)}, H_1), \quad (18)$$

where the likelihood above is given by (8) and $\hat{A}_k^{(j)}$ denotes the ML estimation of $A_k^{(j)}$.

For the sake of simplicity in notation, we denote the $i_k^{(j)}$th data vector $Z_k(i_k^{(j)})$ by Z_k in this section. After taking the natural logarithm of (8), we obtain

$$\begin{aligned} &\log l(Z_k|X_k^{(j)}, A_k^{(j)}, H_1) = \\ &- Z_k^H (\sigma^2\mathbf{I})^{-1} Z_k + 2\Re\left({A_k^{(j)}}^* \mathrm{s}_k(\theta_k^{(j)}, r_k^{(j)}, \omega_{d_k}^{(j)})^H (\sigma^2\mathbf{I})^{-1} Z_k\right) \\ &- |A_k^{(j)}|^2 \mathrm{s}_k(\theta_k^{(j)}, r_k^{(j)}, \omega_{d_k}^{(j)})^H (\sigma^2\mathbf{I})^{-1} \mathrm{s}_k(\theta_k^{(j)}, r_k^{(j)}, \omega_{d_k}^{(j)}). \quad (19) \end{aligned}$$

where $(.)^*$ denotes complex conjugation, $(.)^H$ is the Hermitian transpose, and, $\Re(.)$ takes the real part of its complex argument. The partial derivative of (19) with respect to $A_k^{(j)}$ is given by

$$\frac{\partial \log l(Z_k|X_k^{(j)}, A_k^{(j)}, H_1)}{\partial A_k^{(j)}} = 2\mathrm{s}_k(\theta_k^{(j)}, r_k^{(j)}, \omega_{d_k}^{(j)})^H(\sigma^2\mathbf{I})^{-1}Z_k$$
$$- 2A_k^{(j)}\mathrm{s}_k(\theta_k^{(j)}, r_k^{(j)}, \omega_{d_k}^{(j)})^H(\sigma^2\mathbf{I})^{-1}\mathrm{s}_k(\theta_k^{(j)}, r_k^{(j)}, \omega_{d_k}^{(j)}). \tag{20}$$

The ML solution in (18) is found by setting (20) to zero, i.e.,

$$\frac{\partial \log l(Z_k|X_k^{(j)}, A_k^{(j)}, H_1)}{\partial A_k^{(j)}} = 0$$

which is satisfied at

$$\hat{A}_k^{(j)} = \frac{s_k(\theta_k^{(j)}, r_k^{(j)}, \omega_{d_k}^{(j)})^H(\sigma^2\mathbf{I})^{-1}Z_k}{s_k(\theta_k^{(j)}, r_k^{(j)}, \omega_{d_k}^{(j)})^H(\sigma^2\mathbf{I})^{-1}s_k(\theta_k^{(j)}, r_k^{(j)}, \omega_{d_k}^{(j)})}, \tag{21}$$

where $s_k(\theta_k^{(j)}, r_k^{(j)}, \omega_{d_k}^{(j)}) \in \mathbb{C}^{LN\times 1}$ is the noise free spatio-temporal vector found by evaluating (3) at $X_k^{(j)}$, $\sigma^2\mathbf{I} \in \mathbb{R}^{LN\times LN}$ is the noise covariance, $Z_k \in \mathbb{C}^{LN\times 1}$ corresponds to the measurements in the k^{th} CPI from the bearing-range-doppler bin of $X_k^{(j)}$ (i.e., $i_k^{(j)}$), and $\hat{A}_k^{(j)} \in \mathbb{C}^{1\times 1}$ is the estimated reflection coefficient.

Next, we substitute the ML estimate given in (21) together with $X_k^{(j)}$ in (8) and (15) so as to update the weights of the particles. Here, the term in the numerator of (21) provides coherent integration of $L \times N$ measurement samples.

C. Long time integration for detection

Now let us consider long time integration in order to decide on the object existence. The integration described above can integrate reflection coefficient from $k = 1$ to K and also take into account the estimated object state $\hat{X}_{1:K}$. We substitute the estimate of the kinematic parameters $\hat{X}_k$ found by using the SMC recursions and (16) in (21). This results with the ML estimate of the reflection coefficient $\hat{A}_k$ at $\hat{X}_k$, i.e.,

$$\hat{A}_k = \frac{s_k(\hat{\theta}_k, \hat{r}_k, \hat{\omega}_{d_k})^H(\sigma^2\mathbf{I})^{-1}Z_k}{s_k(\hat{\theta}_k, \hat{r}_k, \hat{\omega}_{d_k})^H(\sigma^2\mathbf{I})^{-1}s_k(\hat{\theta}_k, \hat{r}_k, \hat{\omega}_{d_k})}. \tag{22}$$

After obtaining $\hat{X}_k$ and $\hat{A}_k$ for $k = 1, \ldots, K$, we substitute these values in (the natural logarithm of) (10) and the likelihood ratio test in (6). The detection test is performed by

$$\log L(Z_{1:K}|\hat{X}_{1:K}, \hat{A}_{1:K}) \underset{H_0}{\overset{H_1}{\gtrless}} \log \mathcal{T}_k \tag{23}$$

Doing so provides coherent integration of $L \times N$ samples within a CPI, and, non-coherent integration across CPIs by taking into account $\hat{X}_{1:k}$. Here, $\log \mathcal{T}_k$ is a CFAR threshold for the log-likelihood ratio at the k^{th} step.

D. Constant false alarm rate threshold

The CFAR detection threshold $\mathcal{T}_k$ can be calculated as a function of the selected probability of false alarm P_{fa}. First, the likelihood of the noise only signal hypothesis in (9) is considered, which can be written as

$$p(Z_k|H_0) = \frac{1}{\pi k\sigma^2}\exp\left(-\frac{|Z_k|^2}{k\sigma^2}\right), \tag{24}$$

where Z_k is the k^{th} measurement. Second, the P_{fa} of a threshold test is given by the integration of $p(Z_k|H_0)$ when Z_k is over a threshold $\mathcal{T}_k$. In other words,

$$P_{fa} = \int_{\mathcal{T}_k}^{+\infty} p(Z_k|H_0)dZ_k = \frac{1}{\pi\sigma\sqrt{k}}\int_{\frac{\mathcal{T}_k}{\sqrt{k\sigma^2}}}^{+\infty}\exp\left(-|t|^2\right)dt$$
$$= \frac{1}{2\sigma\sqrt{\pi k}}\mathrm{erfc}\left(\frac{\mathcal{T}_k}{\sqrt{k\sigma^2}}\right), \tag{25}$$

where $\mathrm{erfc}(.)$ is the complementary error function (see, e.g., [1, Chp.6]). The detection threshold $\mathcal{T}_k$ at the k^{th} step of integration is calculated by

$$\mathcal{T}_k = \sqrt{k\sigma^2}\mathrm{erfc}\left(2\sigma\sqrt{\pi k}P_{fa}\right)^{-1}, \tag{26}$$

where $\mathrm{erfc}(.)^{-1}$ is the inverse complimentary error function. Given a false alarm rate, we now have an expression for the threshold value of the likelihood ratio test in (23).

IV. Example

In this section, we demonstrate the proposed detection approach through an example. We consider a scenario in which a single pulsed radar transmitter emits $N = 20$ linear frequency modulated (i.e., chirp) waveforms during a CPI. A single object with initial sate $X_0 = [1000\mathrm{m}, 1000\mathrm{m}, 60\mathrm{m/s}, 10\mathrm{m/s}]^T$ moves along an unknown trajectory across consecutive CPIs in accordance with the manoeuvring object dynamic model using (14). A co-located ULA receiver receives reflected versions of the transmitted pulses with the signal model in (5). Table I shows the parameters of the transmitted pulses used in this scenario. Based on these parameters, the bearing resolution can be found as $\Delta\theta = 5.1^\circ$ using $\Delta\theta = 2\sin^{-1}\left(\frac{0.891}{L}\right)$ (see, e.g., [10]) and the range resolution is found using the formula $\Delta r = c/2B$ as 150m. This is illustrated in Fig. 2, where the blue and red dashed lines indicate the bearing resolution and the range resolution boundaries, respectively. Furthermore, the velocity resolution ΔV given by $\frac{\lambda_c}{2NT}$ is found as 7.5m/s (or, equivalently the doppler resolution is $\Delta\omega = 4\pi f_c\frac{\Delta V}{c}T$ which evaluates as $0.314\mathrm{deg/s}$).

We apply the proposed algorithm for testing object existence on range-bearing and velocity bins with $M = 600$ particles initially selected as a 30×20 element uniform grid within the

TABLE I
TRANSMITTED SIGNAL PARAMETERS

Parameter	Value
Carrier frequency f_c	10GHz
Bandwidth B	1MHz
Pulse repetition interval T	100us
Coherent processing interval (CPI) Δ	0.1s
Number of pulses during a CPI N	20
Number of elements on ULA L	20

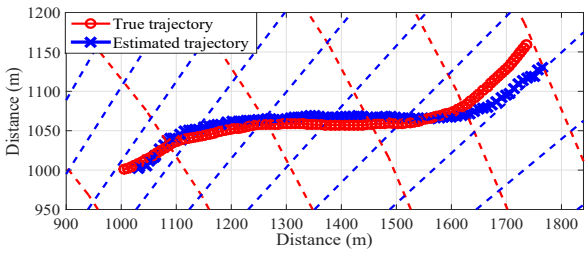

Fig. 2. Example scenario: A -2dB object follows a trajectory (red line) across range-bearing bins (separated by dashed lines). The proposed algorithm simultaneously estimates the trajectory (blue line) and performs a likelihood ratio test for detection.

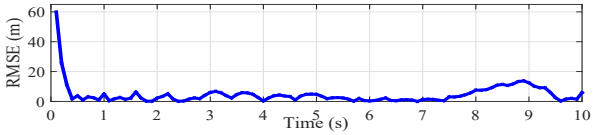

Fig. 3. RMSE of the trajectory estimate obtained by using the proposed algorithm in a typical experiment with a -2dB SNR manoeuvring object.

bin under test. We also use the proposed algorithm for long time integration spanning 10s with a CPI interval of 0.1s. The reflection coefficient is generated from a complex Gaussian density leading to an expected SNR of -2dB.

In this example, when the bin under test contains an object, the particles converge to the underlying state, the integrated value rises above the CFAR threshold, and the algorithm detects the object. When there is no object, the particles lead to a low likelihood value for object existence. A typical estimated trajectory is given in Fig. 2 (blue crossed line). The estimated trajectory is reasonably close to the true trajectory (red line). The root mean square error (RMSE) of this estimate is given in Fig. 3, which indicates a reasonably low value after only a few steps (equivalently, CPIs).

Now, let us consider pulse integration and detection using the proposed method. We generate 100 measurement sets for the scenario described (Fig. 2) and compare the long time-integration value obtained using the proposed algorithm with the best integration achievable if the true trajectory of the object was known. Fig. 4 illustrates the average long-time integration value (solid blue line) with ± 1 standard deviation bounds (dash dotted lines). The average integrated energy reaches a value of 56.5 at $t = 10$s which is very close to the best achievable result using the true object trajectory (dashed red line). Next, we consider the CFAR threshold (solid magenta line) calculated using (26) for $P_{fa} = 10^{-8}$. It is seen that in all simulations, the proposed algorithm yields an integration value that exceeds the CFAR threshold and reports object detection. Conventional integration methods, i.e., coherent (black line) and non-coherent (green line) integration fail to exceed the CFAR threshold and detect the object, in all experiments.

Next, we consider probability of the detection P_d as a function of time. We calculate this probability for the proposed algorithm empirically and depict in Fig. 5 in comparison with integration using the true object trajectory. The P_d for the proposed approach (solid blue line) increases over time, as

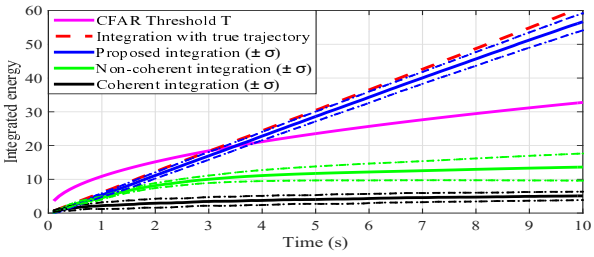

Fig. 4. Long time-integration with the proposed algorithm: The integrated value (solid blue line) versus time (dash-dotted lines indicate ± 1 standard deviation σ bounds), the best achievable integration using the true trajectory (dashed red line) and the CFAR threshold (solid magenta line). Conventional non-coherent (green line) and coherent (black line) integration fail to exceed the detection threshold. The results are averaged over 100 MC simulations.

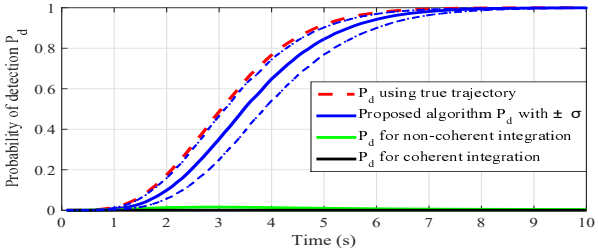

Fig. 5. Probability of detection (P_d) versus time in 100 MC simulations: The proposed long time integration algorithm (solid blue line and $\pm\sigma$ bounds rendered with blue dashed-lines), the best achievable P_d with integration using the complete knowledge of the true trajectory (red dashed line), non-coherent integration (green), and coherent integration (black).

more returns from the object is integrated. Note that the rate of increase is very similar to the P_d using true trajectory (red dashed line). It exceeds 0.5 after $t = 3.5$s and reaches almost 1 by $t = 7$s. Conventional non-coherent and coherent integrations yield zero P_d, in this scenario.

V. Conclusion

In this work, we proposed a joint pulse integration and trajectory estimation algorithm for detecting low SNR manoeuvring targets. This algorithm allows us to estimate the reflected pulse energy for each possible state and then add them using coherent integration during a CPI. We also use non-coherent integration across consecutive CPIs. This integration approach results in an integrated value close to the best achievable if we had full knowledge of the true trajectory. Future work includes further experimentation for the characterisation of the algorithm under different SNR working conditions.

Acknowledgement

This work was supported by the Engineering and Physical Sciences Research Council (EPSRC) grants EP/J015180/1 and EP/K014277/1, and the MOD University Defence Research Collaboration (UDRC) in Signal processing.

References

[1] M. Richards, *Fundamentals of Radar Signal Processing*, ser. Professional Engineering. Mcgraw-hill, 2005.

[2] X. Chen, J. Guan, N. Liu, and Y. He, "Maneuvering target detection via radon-fractional fourier transform-based long-time coherent integration," *IEEE Trans. Sig. Proc.*, vol. 62, no. 4, pp. 939–953, Feb 2014.

[3] Y. Boers and J. Driessen, "Multitarget particle filter track before detect application," *IEE Proceedings on Radar, Sonar and Navigation*, vol. 151, no. 6, pp. 351–357, Dec 2004.

[4] E. Grossi, M. Lops, and L. Venturino, "A novel dynamic programming algorithm for track-before-detect in radar systems," *IEEE Trans. Sig. Proc.*, vol. 61, no. 10, pp. 2608–2619, May 2013.

[5] M. Uney, B. Mulgrew, and D. Clark, "Maximum likelihood signal parameter estimation via track before detect," in *Sensor Signal Processing for Defence (SSPD), 2015*, Sept 2015, pp. 1–5.

[6] S. Davey, M. Rutten, and B. Cheung, "Using phase to improve track-before-detect," *IEEE Transactions on Aerospace and Electronic Systems*, vol. 48, no. 1, pp. 832–849, Jan 2012.

[7] O. Rabaste, C. Riche, and A. Lepoutre, "Long-time coherent integration for low snr target via particle filter in track-before-detect," in *15th Int. Conf. Information Fusion (FUSION)*, July 2012, pp. 127–134.

[8] S. Kay, *Fundamentals of Statistical Signal Processing: Detection theory*, ser. Prentice Hall Signal Processing Series. Prentice-Hall PTR, 1998.

[9] M. Arulampalam, S. Maskell, N. Gordon, and T. Clapp, "A tutorial on particle filters for online nonlinear/non-gaussian bayesian tracking," *IEEE Trans. Sig. Proc.*, vol. 50, no. 2, pp. 174–188, Feb 2002.

[10] H. L. Van Trees, *Optimum Array Processing*. John Wiley & Sons, Inc., 2002, ch. 2, Arrays and Spatial Filters, pp. 17–89.